NMR Spectra of the Porphyrins. Part 40.[1] Self-aggregation in Zinc(II) and Nickel(II) 2-Vinylphylloerythrins

Raymond J. Abraham,*[,a] Alan E. Rowan,[a] Kathryn E. Mansfield[b] and Kevin M. Smith*[,b]
[a] *The Chemistry Department, The University of Liverpool, P.O. Box 147, Liverpool, L69 3BX, UK*
[b] *Department of Chemistry, University of California, Davis, CA 95616, USA*

The large concentration dependence of the ^{1}H NMR spectrum of nickel(II) 2-vinylphylloerythrin has been recorded and analysed in terms of both monomer–dimer and monomer–dimer–trimer equilibria. The equilibrium constant obtained from these analyses is *ca.* 250 dm^3 mol^{-1} which is large enough to give significant concentration shifts at concentrations of 2×10^{-4} mol dm^{-3}.

The complexation shifts are almost identical to those obtained previously for zinc(II) 2-vinylphylloerythrin, showing, in this porphyrin, the independence of the aggregate structure to the central metal atom.

The aggregation shifts obtained were analysed using a previous well-defined ring-current model and considering all possible modes of aggregation, including face-to-face and back-to-face structures. The aggregation shifts are best reproduced on the basis of a model in which the porphyrin ring current is reduced by *ca.* 5% on aggregation. In this model the separation of the porphyrin planes is *ca.* 5.0 Å with some lateral displacement. Both face-to-face and back-to-face structures give almost identical calculated shifts in complete agreement with the observed shifts.

The aggregation behaviour of porphyrins and chlorophylls has been well reviewed[2–4] and intensively studied, in previous parts of this series[5,6] and elsewhere,[7,8] as this behaviour is of both practical and intrinsic importance in porphyrin chemistry. Even simple characterisation of the NMR spectra of metalloporphyrins can be hazardous if the complexation tendencies of the molecules are not considered,[9] furthermore, a knowledge of the mechanism of aggregation may lead to a better understanding of the chemistry of metalloporphyrins, and particularly chlorophylls, *in vivo*.[3,10] In the porphyrins, three types of aggregation have been proposed.[9,11] (*i*) A weak π–π aggregation in free base porphyrins. (*ii*) A stronger π–π aggregation in metalloporphyrins. (*iii*) In some cases a strong metal to side chain complexation.

The geometry of the first two is of interest, in that the preferential stacking of these large flat molecules is *via* an offset geometry rather than one vertically above the other, in both the free bases and the metalloporphyrins. Introduction of the metal increases the strength of the binding but does not affect the geometry and this has been observed in both inter- and intramolecular complexation.[7] A very useful summary of porphyrin

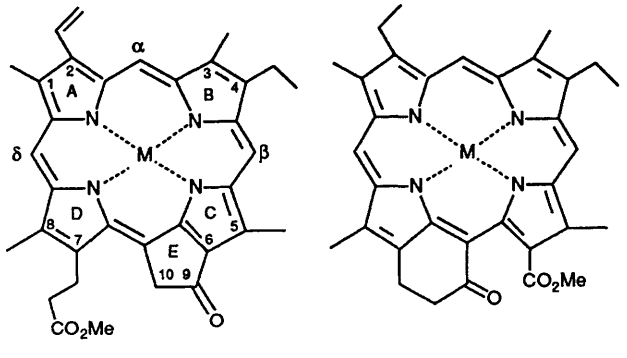

1a M = Zn
b M = Ni

2a M = Zn
b M = Ni

Fig. 1 Structure (Fischer numbering) of 2-vinylphylloerythrin (**1**) and anhydro-rhodoporphyrin XV methyl ester (**2**)

interactions combined with a quantitative rationalisation of most of the above trends has recently appeared.[11a]

In previous parts of this series the aggregation of the zinc 2-vinylphylloerythrin (**1a**) was investigated by ^{1}H NMR spectroscopy,[6] using pyridine to break up the aggregates by competitive binding to the zinc, and a ring-current model to analyse the observed proton shifts. More recently, in an investigation of the ring current in anhydroporphyrins,[12] it was observed that although the corresponding nickel 2-vinylphylloerythrin (**1b**) also showed aggregation shifts, the proton spectrum being affected by dilution, the very similar molecule nickel anhydro-*meso*-rhodoporphyrin XV methyl ester (**2b**), and also the corresponding nickel chlorins, showed no evidence of aggregation. The ^{1}H NMR spectrum was completely unchanged upon dilution. It was therefore of some interest to investigate the aggregation behaviour of **1b** in more detail, in order to try and identify those characteristics which were responsible for the very different behaviour of compounds **1** and **2**.

As nickel porphyrins (unlike the corresponding zinc porphyrins) do not form diamagnetic complexes with extraneous ligands (the addition of strong bases *e.g.*, pyridine causes the hybridisation to change from planar to tetrahedral and in consequence the metal becomes paramagnetic[13]), the only method of obtaining the complexation shifts is by analysis of the proton chemical shifts *vs.* dilution plots. Here we give the complete assignment of the proton spectrum of **1b** together with the analysis of the observed dilution equilibria. The aggregation shifts obtained are analysed using the refined ring-current model and the resulting aggregate structure considered with respect to both the analogous zinc complex and the similar nickel compound **2**.

Theory.—The ring-current model used has been described previously,[5,6] thus only a brief summary is given here. The porphyrin macrocyclic ring current is broken down into smaller current loops which are then replaced by their equivalent dipoles. The parameterisation for the zinc (**1a**) and nickel porphyrins given previously[6] [μ_p 16.1, μ_h 18.1 (pyrrole and hexagon dipoles)] may be used for **1b**, and for the intermolecular distances considered subsequently (*ca.* 4–6 Å), the

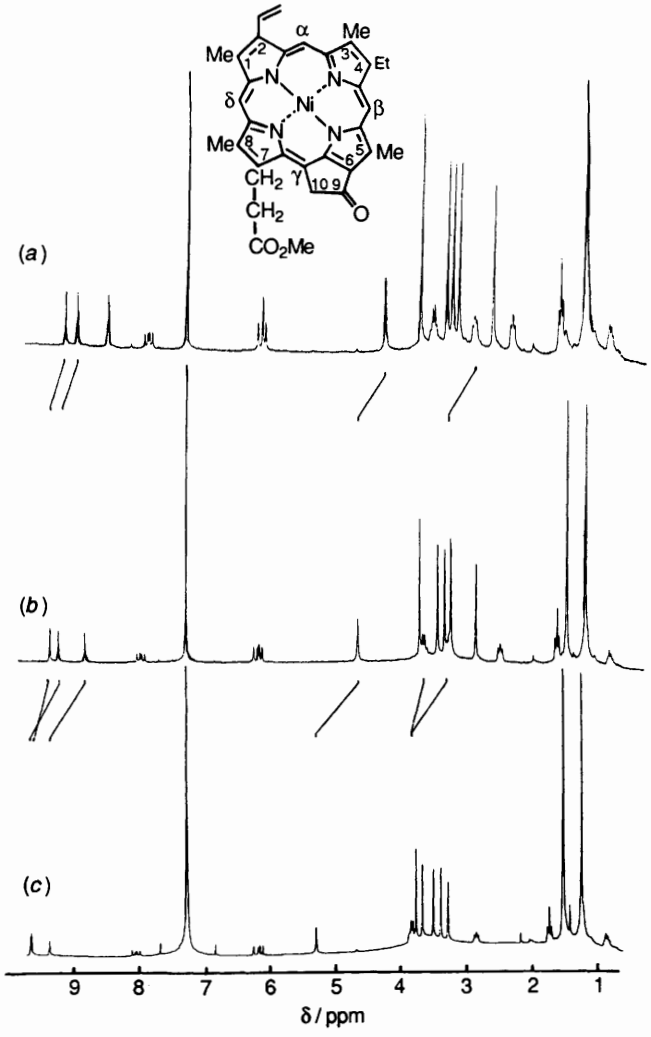

Fig. 2 ^{1}H NMR spectra of nickel(II) vinylphylloerythrin at various concentrations: (*a*) 17.7 × 10^{-3} mol dm^{-3}; (*b*) 3.5 × 10^{-3} mol dm^{-3}; (*c*) 0.59 × 10^{-3} mol dm^{-3}

short range approximation is not required. As in previous applications in this series, the calculations are restricted to aggregate structures in which the planes of the macrocycles are parallel. This is both convenient and generally accepted, but nevertheless an assumption. The program has been further developed than when first applied to zinc 2-vinylphylloerythrin,[14] and can now handle (within the restriction of parallel-plane dimer complexes) any type of aggregate. This includes, for a dimer complex, a two-fold symmetric dimer which is a one molecule calculation, as both molecules of the dimer are equivalent, and face-to-face (both sides) and back-to-face models in which the shifts of each molecule need to be calculated separately. The 'base' molecule, *i.e.*, the porphyrin ring from which the ring-current shift is calculated, is fixed in the *xy* plane of the coordinate system used, with the centre at the origin, the *z*-axis being the four-fold symmetry axis of the porphyrin. If this is labelled molecule A, then the shifts of the molecule B of the dimer due to molecule A are calculated simply from the displacement co-ordinates (*x*, *y*, *z*) and rotation of B about the *z*-axis (θ). Then the program automatically calculates the ring-current shifts of the molecule A due to molecule B by a series of translations and rotations which preserve the dimer geometry but result in molecule B being the base molecule with A displaced and rotated accordingly. The options available allow for the three possible types of structure mentioned above, although in the case of a planar porphyrin molecule face-to-face and back-to-back are equivalent.

The porphyrin aggregates exchange rapidly on the NMR time scale, thus to compare the observed shifts with those calculated, the separate calculated shifts for any proton in molecule A and B are averaged. Also, in order to allow for the possible formation of higher aggregates than the dimer the observed and calculated shifts can be compared directly (*i.e.*, for a dimer) or the calculated shifts can be normalised (*i.e.*, multiplied by an agreement factor) and thus compared with observed shifts.

The computational iteration to the best fit of the observed and calculated (or normalised) shifts is performed by a simple scanning and elimination process. Although computationally much more efficient procedures could be adopted, it was not considered worthwhile to introduce them, particularly as the definition of the aggregate geometry is not particularly striking (see later).

Experimental

The nickel 2-vinylphylloerythrin (NVP) was prepared as previously described,[14] and dissolved in $CDCl_3$ which had been filtered through activated alumina in order to remove traces of acid and water. The solution was diluted by the incremental addition of $CDCl_3$. The spectra were obtained on a Bruker WM 250 (250 MHz, ^{1}H) fitted with an Aspect 2000 computer. Typical operating conditions were: probe temperature 20 °C, sweep width 2.5 kHz, in 8 K data points, zero filling to 16 K, giving a digital accuracy of 0.32 Hz per point (<0.0013 ppm). The pulse width was 7 μs (60° flip), with an acquisition time of 1.5 s. The NOE experiments were carried out on a Bruker AM 200, fitted with an Aspect 3000 computer. The automated NOEDIFF.AU program was used (see Bruker manual part number Z30345), assuming a t_1 relaxation of 0.5 s for the β-methyls (C-1, C-3, C-5 and C-8 methyls).[15]

Results

In order to minimise the formation of aggregates larger than the dimer the NVP spectra were recorded at concentrations from 2 × 10^{-2} mol dm^{-3} to the lowest attainable concentrations of 2 × 10^{-4} mol dm^{-3}. The ^{1}H NMR spectra of NVP showed large complexation shifts upon dilution (Table 1 and Fig. 2).

The proton spectrum of the most dilute species (17.5 × 10^{-5} mol dm^{-3}), Fig. 2(*c*), was assigned by comparison with the proton spectrum of the analogous zinc 2-vinylphylloerythrin (ZVP) monomer, obtained upon the addition of excess pyridine.[14] The similarity between these two sets of chemical shifts suggests that at this concentration the NVP solution consists predominantly of the monomeric species. [The calculated monomeric chemical shifts (see later) differ only slightly from those observed at this concentration, agreeing with this.] The only difficulty in the assignment arose from ambiguity over the assignment of the four β-methyl resonances (C-1, C-3, C-5 and C-8). The remaining methyl, the (**7d**) ester methyl, can easily be distinguished by its smaller line-width and concentration independence compared to the other methyls. The ambiguity in the assignment of the β-methyls was simply resolved by NOE experiments. (This method was previously found to be successful in the assignment of the β-methyls of methyl pyrrochlorophyllide-*a*[5a]). Fig. 3 shows the observed enhancements upon the irradiation of the β-methyl signals. Irradiation of the low-field methyl resonance at δ 3.5 gave an enhancement to the β-*meso* proton (δ 8.9) [Fig. 3(*a*)], confirming it as the C-5 methyl resonance. Irradiation of the resonance at δ 3.3 gave an enhancement of the δ-*meso* proton (δ 8.4) and a small enhancement of the C-2a vinylic proton, hence this resonance must be the C-1 methyl [Fig. 3b)]. The methyl resonance at δ 3.2 upon saturation gave an enhancement to the α-*meso* proton (δ 9.5)

Table 1 Observed proton chemical shifts[a] (δ/ppm) for nickel(II) vinylphylloerythrin methyl ester *versus* concentration (10^{-3} mol dm^{-3})

	Concentration[b]/10^{-3} mol dm^{-3}																					
Proton	17.73	14.78	12.66	11.08	9.85	8.86	8.06	6.82	5.91	4.43	4.47	2.95	2.53	2.09	1.77	1.48	1.26	1.11	0.98	0.81	0.59	0.17
Meso α	9.09	9.12	9.14	9.17	9.18	9.20	9.22	9.24	9.27	9.32	9.37	9.40	9.42	9.45	9.48	9.50	9.53	9.55	9.56	9.59	9.62	9.70
β	8.91	8.95	8.97	9.01	9.02	9.04	9.04	9.09	9.12	9.19	9.26	9.29	9.35	9.37	9.41	9.45	9.49	9.52	9.55	9.59	9.64	9.78
δ	8.44	8.48	8.51	8.55	8.57	8.60	8.62	8.66	8.70	8.79	8.96	8.92	8.95	9.95	9.07	9.12	9.17	9.21	9.24	9.29	9.36	9.55
2a-H	7.83	7.84	7.85	7.87	7.88	7.88	7.90	7.90	7.92	7.94	7.96	7.97	7.98	7.99	8.00	8.01	8.02	8.02	8.03	8.03	8.04	8.05
2b-H	6.15	6.16	6.17	6.17	6.17	6.17	6.18	6.18	6.19	6.20	6.20	6.21	6.21	6.21	6.22	6.22	6.22	6.22	6.22	6.22	6.22	6.22
2b′-H	6.09	6.10	6.10	6.10	6.11	6.13	6.12	6.12	6.12	6.13	6.13	6.13	6.14	6.14	6.14	6.14	6.14	6.14	6.14	6.14	6.14	6.14
10-H_2	4.25	4.30	4.34	4.38	4.40	4.43	4.46	4.51	4.55	4.66	4.75	4.80	4.84	4.92	4.98	5.03	5.09	5.13	5.17	5.22	5.30	5.51
7d-OMe	3.71	3.71	3.71	3.74	3.72	3.72	3.72	3.72	3.72	3.73	3.73	3.73	3.74	3.74	3.74	3.74	3.75	3.75	3.75	3.75	3.76	3.76
5-Me	3.51	3.53	3.55	3.56	3.57	3.59	3.60	3.62	3.63	3.66	3.69	3.71	3.72	3.74	3.75	3.76	3.78	3.79	3.79	3.81	3.82	3.85
1-Me	3.32	3.34	3.35	3.37	3.37	3.39	3.40	3.41	3.43	3.46	3.49	3.51	3.52	3.54	3.56	3.58	3.59	3.61	3.62	3.64	3.66	3.72
3-Me	3.24	3.25	3.27	3.28	3.29	3.29	3.30	3.32	3.33	3.36	3.38	3.39	3.40	3.42	3.43	3.44	3.45	3.46	3.47	3.48	3.49	3.52
4a-H_2	3.15	3.16	3.17	3.19	3.19	3.20	3.21	3.23	3.24	3.27	3.29	3.30	3.30	3.32	2.33	3.34	3.35	3.35	3.36	3.37	3.38	3.39
7a-H_2	2.91	2.96	2.99	3.03	3.05	2.09	3.11	3.16	3.19	3.29	3.37	3.44	3.46	3.54	3.58	3.62	3.67	3.71	3.75	3.79	3.82	3.01
8-Me	2.64	2.67	2.69	2.72	2.73	2.76	2.77	2.80	2.72	2.90	2.95	2.99	3.01	3.05	3.09	3.12	3.15	3.17	3.20	3.23	2.26	3.38
7b-H_2	2.34	2.37	2.38	2.40	2.41	2.43	2.44	2.46	2.40	2.53	2.58	2.60	2.62	2.66	2.69	2.71	2.74	2.76	2.78	2.81	2.84	2.94
4b-Me	1.63	1.63	1.64	1.64	1.65	1.65	1.66	1.66	1.64	1.68	1.69	1.69	1.70	1.71	1.71	1.72	1.72	1.72	1.73	1.73	1.74	1.75

[a] All chemical shifts referenced to TMS. [b] Initial concentration 1.77×10^{-2} mol dm^{-3} (4.85 mg in 0.5 cm^3).

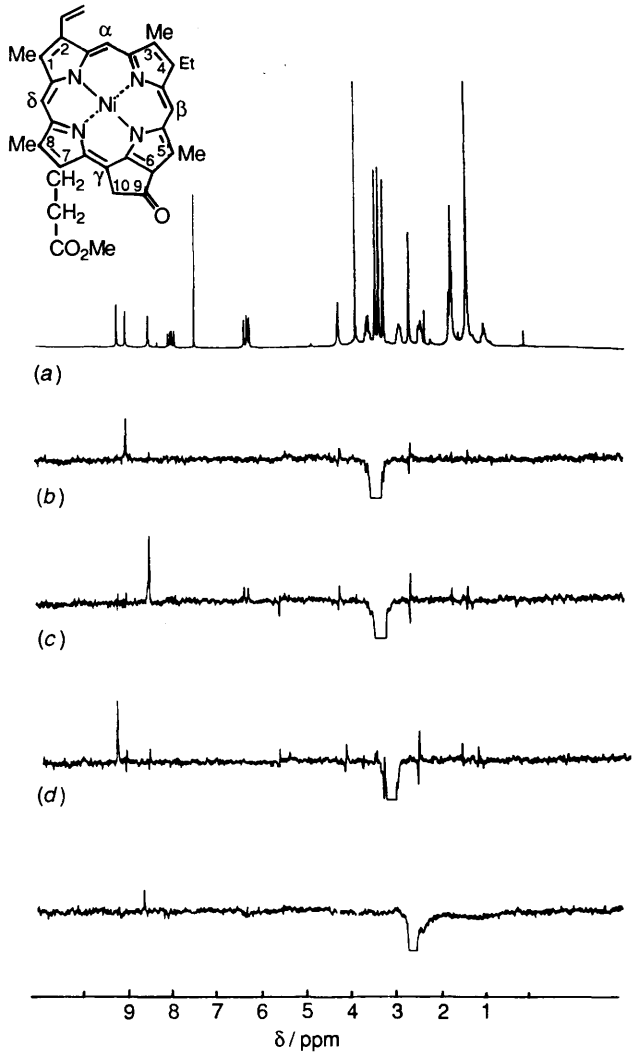

Fig. 3 NOEs observed upon the irradiation of (*a*) 5-Me, (*b*) 1-Me, (*c*) 3-Me, (*d*) 8-Me proton resonances of nickel(II) vinylphylloerythrin (17×10^{-3} mol dm^{-3})

confirming it as the C-3 methyl [Fig. 3(*c*)]. The remaining methyl resonance must be that of the C-8 methyl and this is confirmed by the observed enhancement, upon irradiation, of the *δ-meso* proton at δ 8.4 [Fig. 3(*d*)].

The assignment of the remaining resonances in the aggregate spectra follows directly from that of the disaggregate. It can be seen that upon dilution some crossing of resonances occurs (Fig. 2), one of the most prominent being the crossing of the β-*meso* proton, with the α-*meso* proton [Fig. 2(*a*)]. Other resonances also show remarkable complexation shifts. The most noticeable is the C-7a methylene triplet which, upon dilution, moves downfield from δ 2.91 to 4.01 (see Table 1) crossing over all the β-methyls, the C-7d methyl and eventually the C-4a quartet (which also crosses the C-7d methyl). It is worth noting that the C-7d methyl has very little complexation shift which implies that the side-chain plays no role in the binding mechanism and sticks out into the solvent.

The complexation shifts [δ(monomer) − δ (dimer)] were obtained by analysis of the aggregate–disaggregate equilibrium. If this equilibrium is considered to be due solely to a monomer–dimer equilibrium [according to eqn. (1)], the observed shift of any given proton is the weighted average of the corresponding shifts in the dimer (δ_d) and the monomer (δ_m), given by eqn. (3) where x [eqn. (1)] is the fraction of the monomer converted into

$$\underset{(1-x)}{2\text{NVP}} \overset{K_1}{\rightleftharpoons} \underset{x/2}{(\text{NVP})_2} \quad (1)$$

$$\underset{1-y}{\text{NVP}} + \underset{y}{(\text{NVP})_2} \overset{K_2}{\rightleftharpoons} (\text{NVP})_3 \quad (2)$$

$$\delta_{obs} = (1 - x)\delta_m + 2(x/2)\delta_d \quad (3)$$

dimer. Combining eqns. (1) and (3) gives the observed shift as a function of the monomer and dimer chemical shifts and the equilibrium constant [eqn. (4)], where K is the equilibrium

$$\delta_{obs} = \delta_m + (\delta_d - \delta_m)[1 + 4aK - (1 + 8aK)^{\frac{1}{2}}]/4aK \quad (4)$$

constant and a is the concentration. A consequence of this analysis is that the concentration dependence of any one proton is linearly related to that of all the other protons. This indeed was found to be so, and the δ values in Table 1 were all plotted against those of the C-10 methylene protons to give good linear correlations (all correlation coefficients $\geqslant 0.99$ except for those protons with little concentration dependence). Thus we only need to analyse one curve, and we will use the C-10 methylene protons, as these have the largest concentration dependence. An iterative analysis of the dilution plot for the C-10 methylene

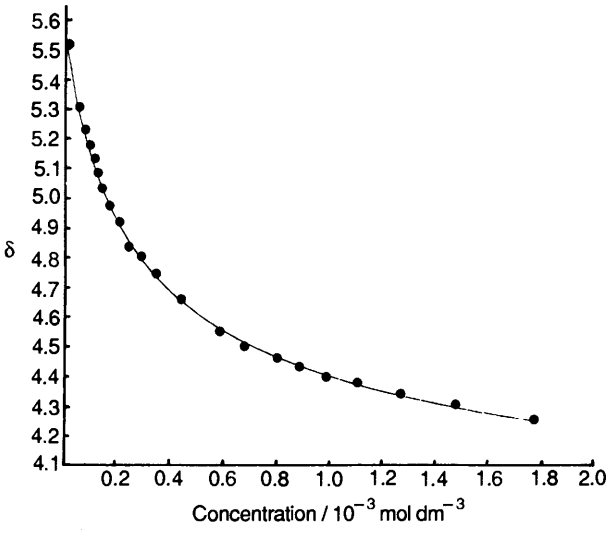

Fig. 4 Plot of ^{1}H chemical shift *versus* concentration for the 10-CH_2 resonances. Observed points and calculated curve (rms error = 0.006) (δ_d 3.65 ppm, δ_m 5.65 ppm for monomer–dimer equilibria; δ_d 4.30 ppm, δ_m 5.60 ppm for monomer–dimer–trimer equilibria).

protons according to eqn. (4), (varying the three unknowns δ_m, δ_d and K) gave the best solution with an rms error of 0.006 ppm, with K = 225 dm^3 mol^{-1} and δ_m and δ_d values of 5.65 and 3.65 respectively, *i.e.*, a complexation shift ($\Delta\delta$) for the C-10 methylene protons of 2.00 ppm. Fig. 4 shows the calculated curve and the observed chemical shifts for the C-10 methylene protons.

The excellent agreement of Fig. 4 is, however, somewhat misleading as a range of solutions can be obtained, all with acceptable rms errors. This range of solutions can be restricted by fixing δ_m by simple extrapolation of the observed plot to zero concentration, which gives a value of δ_m 5.63, almost identical with the best solution above. This two-parameter equation still gives a range of acceptable solutions, *e.g.*, with δ_d equal to 4.0 and K 360 dm^3 mol^{-1} the rms error is 0.06 ppm, still within acceptable limits.

Thus, analysis of the dilution curves on the basis of the monomer–dimer equilibrium gives a range of solutions with δ_d 3.6–4.0 ppm and K 220–360 dm^3 mol^{-1}. It was also found that the calculated complexation shift, assuming this simple monomer–dimer equilibrium, could not be calculated directly using the ring-current model (see later), but needed to be multiplied by a normalisation factor in order to obtain agreement. This implied that the initial aggegate solution had a significant percentage of the larger trimer aggregate present.

Many previous workers have deduced the presence of large aggregates in such metalloporphyrin solutions. A good example is given by the very well-documented case of chlorophyll-a, in which the aggregation number is two in solutions <0.01 mol dm^{-3} increasing to *ca.* four in 0.1 mol dm^{-3} solutions. Chlorophyll-b aggregates even more strongly than chlorophyll-a, with 'a trimer–hexamer equilibrium in which the hexamer becomes important in solutions more concentrated than 0.01 mol dm^{-3}.'[6,16]

Consequently the dilution data was analysed again, this time assuming the presence of the second equilibrium *i.e.*, eqn. (2), as well as the first. In this case y is the mole fraction of dimer converted to trimer. The observed chemical shift is now also a function of the trimer chemical shift (δ_t) and is given by eqn. (5)

$$\delta_{obs} = n_1\delta_m + 2n_2\delta_d + 3n_3\delta_t \quad (5)$$

where n_1, n_2 and n_3 are the mole fractions of each species. In order to analyse this more complex equilibrium it is necessary to make some simplifying assumptions to reduce the number of unknowns. We assume that $K_1 = K_2$, *i.e.*, the association of a third molecule takes place in exactly the same manner as that of the dimer. The second assumption is that the trimer complexation shift ($\delta_t - \delta_m$) is equal to 1.5 × ($\delta_m - \delta_d$). This assumption holds true if the formation of the trimer occurs by the same binding geometry, and consequently the same binding mechanism, as that present in the dimer. Assuming the above, the observed shifts can be given by eqn. (6), *i.e.*, in terms of the three

$$\delta_{obs} - \delta_m = \{\delta_d - \delta_m[x(1 + y) + 4.5(xy)]\} \quad (6)$$

unknowns δ_m, δ_d and K. Iterative analysis of the dilution plot for the C-10 methylene protons gave good agreement (rms error 0.006), with a calculated equilibrium K ($K_1 = K_2$) of 255 mol dm^{-3}, and monomer and dimer shifts of 5.60 and 4.20, respectively (the trimer shift being 3.65). The inclusion of the presence of the trimer in the equilibrium significantly reduces the calculated complexation shifts (1.30 ppm) compared to those calculated assuming the simple monomer–dimer equilibrium (1.4–2.00 ppm). The estimated complexation shift for the C-10 protons (1.3 ppm) is fortuitously very similar to the observed dilution shift given previously for ZVP[6] (1.26 ppm). It is therefore convenient to compare both ZVP and NVP and analyse these observed dilution shifts directly (Table 2), as described below.

The Aggregate Structure.—The observed relative dilution shifts for ZVP[6] and NVP are compared in Table 2, and it can be seen that the agreement is complete. This is of some interest in that the dilution shifts, and therefore the aggregate geometry, is not a function of the particular metal in this metalloporphyrin. The ZVP dilution shifts were analysed previously assuming only a symmetric dimer (*i.e.*, a one-molecule calculation) and good agreement between the observed and calculated shifts was obtained from a normalised calculation.[6]

The one-molecule calculations could not, however, distinguish between two possible modes of aggregation, a centrosymmetric dimer Fig. 5(*a*) and a two-fold symmetric dimer Fig. 5(*b*) as these gave identical calculated shifts. As the program can now handle both these structures it was of interest to consider all the possible modes of aggregation to see whether the extent of the agreement could distinguish between them. We note that the general face-to-face and back-to-face structures [which are the general structures of which Fig. (*a*) and (*b*) are particular representations] will not necessarily possess any symmetry.

The 'one-molecule' calculation is only an approximation, as it assumes that the dimer has either a two-fold axis of symmetry or a centre of symmetry. This is only true for displacements in the xy plane which do not involve any rotation of the molecule. As this calculation is included in the more general face-to-face and back-to-face structures we will not consider it separately any further.

In Table 2 are given the observed shifts for ZVP and NVP, together with the calculated shifts obtained from a computational search for the best agreement factor on the basis of three different treatments of this data. We consider first the face-to-face structure (the back-to-face structure will be dealt with subsequently). The observed shifts for NVP (Table 2) were used as input for the iterations, although those for ZVP would give identical conclusions. Also, only the protons of well-defined geometry were used in the search procedures, *i.e.*, the *meso* protons, the β-methyls and the C-10 methylene protons. The protons in the side-chains can be included after the dimer geometry is established, with the side-chain orientation varied for the best agreement with the observed shifts. These are

Table 2 Observed and calculated complexation shifts ($\Delta\delta$/ppm) for zinc(II) and nickel(II) 2-vinylphylloerythrin methyl ester

	Observed		Calculated			
			Face-to-face			Back-to-face
Proton	ZVP[a]	NVP[b]	NORM[c]	DIRECT[d]	REDUCE[e]	REDUCE[f]
meso α	0.60	0.61	0.58	0.40	0.56	0.56
β	1.08	0.87	0.88	0.70	0.84	0.81
δ	1.32	1.10	1.09	1.07	1.10	1.13
1-Me	0.23	0.28	0.33	0.18	0.25	0.26
3-Me	0.23	0.25	0.16	0.01	0.12	0.13
5-Me	0.39	0.39	0.47	0.29	0.37	0.41
8-Me	0.73	0.74	0.74	0.55	0.68	0.64
10a-H_2	1.25	1.26	1.24	1.39	1.24	1.22
4a-H_2	0.33	0.34	0.26			
4b-Me	0.15	0.12	0.12			
7a-H_2	0.99	1.11	0.96			
7b-H_2	0.63	0.59	0.63			
7d-Me	0.03	0.05	0.02			
2a-H	0.20	0.23	0.32			
2b-H	0.10	0.07	0.11			
2b'-H	0.02	0.05	0.03			
rms			0.06	0.22	0.06	0.07

[a] Ref. 6. [b] $\delta(17.73 \times 10^{-3}$ mol dm$^{-3}) - \delta(17.5 \times 10^{-5}$ mol dm$^{-3})$, Table 1. Displacement co-ordinates: [c] −0.2, 1.2, 5.8, Θ −30°. [d] 0.4, 1.4, 5.6, Θ −40°. [e] −0.2, 1.4, 5.0, Θ −35°. [f] −0.8, −1.2, 5.0, Θ 215°.

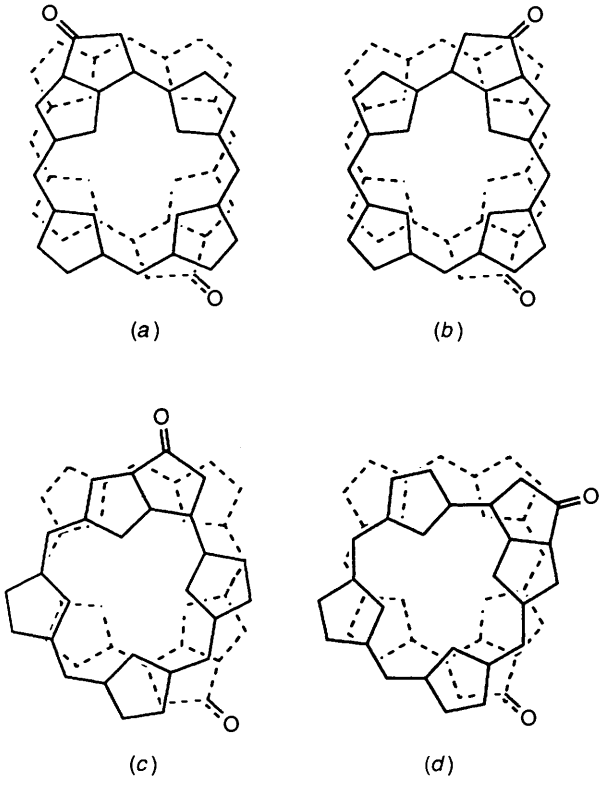

Fig. 5 Calculated dimer structures for nickel(II) vinylphylloerythrin, using normalised shifts. (*a*) Centrosymmetric dimer; (*b*) Two-fold symmetric dimer; (*c*) Face-to-face; (*d*) Back-to-face.

illustrated for one case, full details of these calculations are given elsewhere.[17]

The three separate treatments are: (*a*) the normalised search procedure considered previously,[6] (*b*) an identical search procedure using the observed shifts directly and (*c*) the same procedure as (*b*) but with the inclusion of a 5% reduction in the porphyrin ring current on aggregate formation. The assumptions and limitations of these separate treatments will be discussed at each stage.

The results of the normalised search procedure on the basis of the face-to-face model are given in column 4 of Table 2. This homes, as expected from the results of reference 6, on a good solution with an rms error of 0.07 ppm, well below the experimental uncertainty. The dimer geometry obtained is illustrated in Fig. 5(*d*). This is the general (unsymmetrical) structure which is similar to the two-fold symmetric structure in Fig. 5(*b*). The difference is that one molecule is rotated *ca.* 40° with respect to the other molecule in the dimer. This could not be predicted from the 'one-molecule' calculation. The calculations for the side-chain protons are included in this case and are also in good agreement with the observed shifts, which again would be expected from reference 6.

There are, however, problems with this treatment. The distance between the molecules in the dimer is rather large (5.8 Å) and, more seriously, the normalisation factor is *ca.* 1.5, *i.e.*, the calculated dimer shifts have to be multiplied by this factor to obtain the values in Table 2. This analysis was appropriate in the earlier work[6] as there was at that time no analysis of the observed shifts in terms of the monomer–dimer equilibrium *etc.* However, the results of the previous section show clearly that the observed shifts of Table 2 are good approximations to the actual shifts in the dimer. Certainly the factor of 1.5 is not appropriate.

Thus we next analysed these shifts on the basis of the same face-to-face model but now on a direct treatment without any normalising factor. These results are given in column 5 of Table 2. The solution obtained is virtually identical in geometry to that of the normalised solution, except that the intermolecular separation, as may have been expected, is decreased to 4.6 Å. This is encouraging in that the normalisation procedure appears to give the correct geometry of the aggregate. The agreement for this direct solution is rather poor. The rms error of the observed and calculated shifts is 0.22 ppm, too large to be acceptable. Also, comparison of the observed and calculated shifts is of interest in that all the calculated shifts for this solution are less than the observed shifts, some considerably less. Yet this is the best solution obtained by this treatment, as decreasing the intermolecular separation does not solve this problem and gives poorer solutions.

This intriguing result led us to consider other possibilities. How could the observed aggregate shifts all be greater than the

calculated values? As noted, the solution is not improved if the inter-nuclear separation is decreased, because the ring-current field of the porphyrin is so anisotropic that the peripheral protons now start to experience low-field shifts, giving poorer solutions. It is possible that the act of aggregating two porphyrin molecules could affect their ring currents, since there is considerable interaction between the π systems of the two molecules. Indeed Hunter *et al.*,[11a] in their recent work suggested that the electrostatic interaction between the π electrons of the porphyrins is the dominant mechanism in determining the dimer geometry. Thus it is conceivable that a small decrease in the aromatic ring current could occur on dimer formation. Therefore we give (column 6, Table 2) the results of an identical search to the preceding one except that the ring current of the porphyrin is decreased by 5% on dimer formation. Calculations with different percentage decreases of the ring current gave poorer solutions. The major effect of this is that the protons on the same porphyrin molecule experience an upfield shift which is 0.2 ppm for the *meso* protons and 0.09 ppm for the β-methyl protons. These shifts are subtracted from the observed shifts before the search procedure commences, and then added to the calculated shifts for direct comparison with the observed shifts.

These results are of some interest. Again the geometry of the face-to-face model obtained is identical with that obtained from the other methods, the only change is in the intermolecular separation (5.0 Å), which is slightly larger than in (*b*). What is encouraging is the extent of the agreement. The rms error (0.06 ppm) shows that this treatment provides a complete account of the observed dilution shifts on the basis that these are the dimer shifts. The agreement is excellent for all the observed shifts except for 3-Me. Intriguingly, in the dimer structures obtained [Figs. 5(*c*) and 5(*d*)] the C-3 methyl group is situated over the carbonyl group of the neighbouring molecule. In this orientation the anisotropy of the carbonyl group would be expected to produce an additional high-field shift at the methyl protons[18] which explains the observed deviation.

Precisely similar results to those detailed above for the face-to-face model are obtained for the back-to-face model. Again the normalised solution gives good agreement (rms error 0.08 ppm), the direct calculations much poorer agreement (0.17 ppm) and the direct calculations with 5% reduction in the ring current complete agreement (rms 0.07 ppm). Also, as the geometries for all these solutions only differ in the intermolecular distance (which is in all the cases the same as for the face-to-face solutions given previously), in Table 2 column 7 we give the calculated shifts and geometric parameters only for the last treatment. The full results for the first two cases are given elsewhere.[17]

The geometry obtained for the back-to-face model is shown in Fig. 5(*c*). Although the centrosymmetric structure [Fig. 5(*a*)] is included within this search routine, it is clear that in this case the search homes on a quite different structure. Note that the carbonyl groups in the dimer are not anti-parallel as in Fig. 5(*a*) but in a similar orientation to that of the face-to-face structure [Fig. 5(*c*)].

This result clearly demonstrates the inadequacies of the one-molecule approach, as in the one-molecule calculation the structures in Figs. 5(*a*) and (*b*) give identical calculated shifts.

Discussion

Inspection of the two dimer structures obtained from the search routine [Fig. 5(*c*) and 5(*d*)] shows clearly their general similarity and this is also observed in the calculated shifts (Table 2, columns 6 and 7) which are too similar to be able to distinguish between them.

These structures confirm the previous hypothesis[6] that the most stable aggregate is that in which the electron-deficient pyrrole rings A and C (Fig. 1) overlap with the electron-rich rings B and D. At the intermolecular distances involved (*ca.* 5 Å) the dimer structure will be determined by long range π–π and electrostatic forces,[11a] rather than by localised bonding. The fact that the similar chlorins do not aggregate may be due both to the removal of the electron-rich ring D from the π system (it is saturated in the chlorins) and also to the non-planar substituents. The lack of aggregation in the anhydroporphyrins may also be due to non-planarity of the ring, as the steric interactions between the C-6 methoxycarbonyl substituent and the carbonyl group (Fig. 1) could be severe.

What is of interest about the aggregation in the 2-vinylphylloerythrins is the strength of the aggregation. Even at 10^{-3} mol dm^{-3} the molecules are strongly aggregated in solution.

The equilibrium constant for dimer formation (200–300 dm^3 mol^{-1}) compares with that found in previous studies of zinc protoporphyrin IX (240 dm^3 mol^{-1}) in which a full analysis of the dilution curve was carried out.[19] These results also provide considerable support for the proposed decrease in the ring current on aggregation. In this case both ^1H and ^{13}C dimer shifts were obtained. It was found that although the ^{13}C shifts of the β-methyls correlated closely with the data set of proton dimer shifts (*meso* protons and β substituents), the dimer shifts of the *meso* carbons were much less than expected, and all of them by the same factor (*ca.* 2).

The explanation given was that molecular motions in the dimer structure could be responsible. However, these anomalies can be very simply explained on the basis of a small decrease in the zinc protoporphyrin IX ring current on aggregation. The effect on the *meso* carbon nuclei will be much larger than on the peripheral nuclei and this could give precisely the result obtained. Unfortunately it is not possible on present models to attempt a calculation of the ring-current shift of a *meso* carbon due to the ring current of the same molecule as neither the dipole nor current-loop approximations are likely to be valid at these distances.

The proposed 5% decrease in the ring current on association would also affect ring-current analyses of porphyrin stacking in which the two porphyrin moieties are bound intramolecularly rather than intermolecularly.[7] This decrease has the effect of increasing the estimated inter-porphyrin separation, but only by *ca.* 0.1–0.2 Å, well within the uncertainty in these calculations.

Acknowledgements

This resarch was supported by grants from the National Science Foundation (CHE-90-01381, K. M. S.), the Scientific Affairs Division of NATO (RG 0218/87, R. J. A. and K. M. S.) and the SERC (A. E. R.).

References

1 Part 39, R. J. Abraham, I. Marsden and L. Xiujing, *Magn. Reson. Chem.*, 1990, **28**, 1051.
2 J. J. Katz and H. Scheer, *Porphyrins and Metalloporphyrins*, ed. K. M. Smith, Elsevier, Amsterdam, 1975, pp. 399–524.
3 J. J. Katz, L. L. Shipman, T. M. Cotton and T. R. Janson, *The Porphyrins*, ed. D. Dolphin, Academic Press, New York, 1978, vol. 5, pp. 402–458.
4 R. J. Abraham and A. E. Rowan, *The Chlorophylls*, ed. H. H. Scheer, Verlag Chemie, (in the press).
5 (*a*) R. J. Abraham, A. E. Rowan, D. A. Goff, K. E. Mansfield and K. M. Smith, *J. Chem. Soc., Perkin Trans. 2*, 1989, 1633; (*b*) R. J. Abraham, D. A. Goff and K. M. Smith, *J. Chem. Soc., Perkin Trans. 1*, 1988, 2443; (*c*) K. M. Smith, F. W. Bode, D. A. Goff and R. J. Abraham, *J. Am. Chem. Soc.*, 1986, **108**, 1111.
6 R. J. Abraham and K. M. Smith, *J. Am. Chem. Soc.*, 1983, **105**, 5734.

7 P. Leighton, J. A. Cowan, R. J. Abraham and J. K. M. Sanders, *J. Org. Chem.*, 1988, **53**, 733.
8 R. B. Koehorst, U. Hofstra and T. J. Schaafsma, *Magn. Reson. Chem.*, 1988, **26**, 167.
9 R. J. Abraham, S. C. M. Fell, H. Pearson and K. M. Smith, *Tetrahedron*, 1979, **35**, 733.
10 J. Deisenhofer, O. Epp, K. Miki, R. Huber and H. Micher, *J. Mol. Biol.*, 1984, **180**, 385.
11 (*a*) C. A. Hunter and J. K. M. Sanders, *J. Am. Chem. Soc.*, 1990, **112**, 5525; (*b*) R. J. Abraham, F. Eivazi, H. Pearson and K. M. Smith, *J. Chem. Soc., Chem. Commun.*, 1976, 698.
12 R. J. Abraham, C. J. Medforth, K. E. Mansfield, D. J. Simpson and K. M. Smith, *J. Chem. Soc., Perkin Trans. 2*, 1988, 1365.
13 R. J. Abraham and P. F. Swinton, *J. Chem. Soc. B*, 1969, 903.
14 R. J. Abraham, K. M. Smith, D. A. Goff and J. J. Lai, *J. Am. Chem. Soc.*, 1982, **104**, 4332.
15 F. S. Denniss, J. K. M. Sanders and J. C. Waterton, *J. Chem. Soc., Chem. Commun.*, 1976, 1049.
16 K. Ballschmiter, K. Truesdell and J. J. Katz, *Biochim. Biophys. Acta*, 1969, **184**, 604.
17 A. E. Rowan, Ph.D. Thesis, University of Liverpool, 1991.
18 R. J. Abraham, J. Fisher and P. Loftus, *Introduction to NMR Spectroscopy*, Wiley, New York, 1988, p. 23.
19 R. J. Abraham, S. C. M. Fell, H. Pearson and K. M. Smith, *Tetrahedron*, 1979, **35**, 1759.

Paper 0/04266H
Received 19*th September* 1990
Accepted 19*th November* 1990